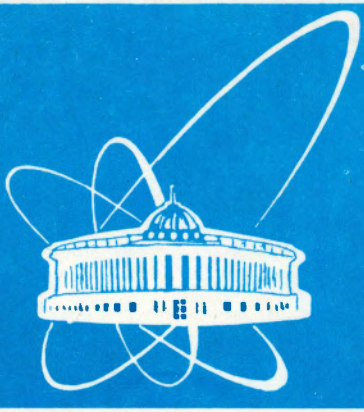

объединенный
институт
ядерных
исследований
дубна

E13-94-214

P.Cantoni[1], P.L.Frabetti[1], L.Stagni[1], P.A.Kulinich,
R.Diaferia[2], S.Parmeggiano[2], B.Maggi[2], F.Lanni[2],
F.Palombo[2], A.Sala[2], P.F.Manfredi[3], V.Re[3], V.Speziali[3]

EXPERIMENTAL STUDY OF PARTICLE SEPARATION IN A LKr IONIZATION CHAMBER BY MULTIPLE MEASURING OF dE/dx USING THE SHAPE ANALYSIS OF SIGNAL

Submitted to «Nuclear Instruments and Methods»

[1]Dipartimento di Fisica dell'Universitá e Sezione INFN, Bologna, Italy
[2]Dipartimento di Fisica dell'Universitá e Sezione INFN, Milano, Italy
[3]Dipartimento di Elettronica dell'Universitá di Pavia e Sezione INFN, Milano, Italy

1994

1 Introduction

The use of liquid medium ionization detectors is attractive due to the possibility of obtaining good energy and spatial resolution. An electromagnetic LKr calorimeter, developed for the KEDR detector, is now under assembling and it will be used at the VEPP-4M e^+e^- collider in Novosibirsk [1]. The KEDR LKr calorimeter consists of a set of ionization chambers operating in the electron-pulse mode, read out by low-noise charge-sensitive preamplifiers.

There should be two detectors in the KEDR setup for particle identification: one using time-of-flight (TOF) information, and the other based on aerogel Cherenkov counters. They should provide particle identification for different secondary particle momentum ranges. To improve (π-k) separation capability of the setup in the intermediate momentum range 0.5÷0.8 GeV/c one can use dE/dx information from the LKr calorimeter chambers. By measuring the momentum of a particle as well as its energy loss, the mass of the particle can be determined. The pulse height information from few consecutive gaps can be used for ordinary dE/dx charged particle (π-k) separation [1]. Such ability of particle identification can improve the performance of the entire setup.

An alternative method of the signal shape analysis was suggested in [2]. This method permits one to reject the parts of the primary charge particle track with energetic delta (δ-) electrons which suppress the right tail of the Vavilov ionization distribution. As Monte Carlo calculation shows, this method can be used at low momentum ($\leq$0.9 GeV/c for π-k separation) of particle depending on the signal to noise ratio. So, the possibility of separating π- and k- mesons at the level of 2σ in a 4 cm LKr medium chamber in the momentum range 0.5÷0.8 GeV/c was shown.

This method permits one to use only one gap signal and, therefore, to decrease the total thickness of liquid media and the disturbance caused by the nuclear interaction.

Some preliminary evaluations of ADC spectra separation were reported in [3]. The results on the experimental studies of the particle separation by the method of shape analysis are described below.

1.1 Beam selection

In order to experimentally study such a possibility, one needs a pion and a kaon beam of low momentum, but the problem is to find the kaon beam of appropriate momentum and suitable particle rate. For study of (π-k) separation at a certain momentum we have used a pion beam of this momentum and a proton beam of a different momentum. The proton beam momentum was calculated in order to have the same velocity as the kaon at the required momentum. Such a proton produces the same ionization loss as the kaon with the momentum equal to that

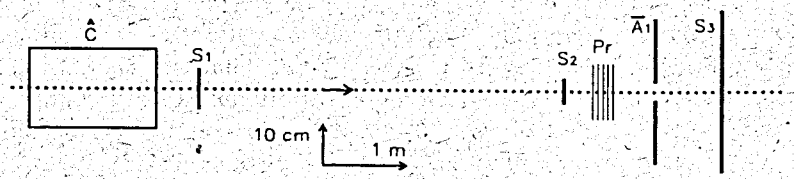

Figure 1: Setup scheme. $\hat{C}$ — Cherenkov counter, $S_1, S_2, S_3, \bar{A}_1$ — scintillator counters, Pr — LKr prototype

of the pion beam [4]. The energy loss in the material along the beam was taken into account in order to obtain the necessary particle momentum at the entrance of the LKr chamber.

We have exposed a prototype of LKr calorimeter to pions and protons in the T11 beam of the CERN PS. The particle contents of this beam can be chosen but, in any case, it is energy dependent and it has significant amount of positrons if the pion beam was chosen, in particular at low energy. Also, the proton beam has a lot of pions, so one should make independent beam particle selection for test studies. For rejection of the positrons in the pion beam and of the pions in the proton beam a gas Cherenkov counter and time-of-flight measurement were used.

The pion beam in the momentum range $0.5 \div 0.8$ GeV/c has a significant admixture of muons, too, because of pion decay. This question was studied by Monte Carlo simulation of our test setup. It was shown that the admixture of muons in the pion beam, which produce the trigger signal, should be about 2% but its ionization spectrum does not practically differ from the pion one.

The beam rate for such application should be set rather low to exclude dynamic saturation of the preamplifiers; we used a beam at a rate around a thousand particles per second.

2 Experimental setup

The experimental setup (Fig. 1) consisted of a beam-defining system and a prototype of LKr calorimeter. The beam was defined by four scintillation counters and a Cherenkov gas counter $\hat{C}$. The anticoincidence counter $\bar{A}_1$ 18×30 cm^2 in size had a 5×5 cm^2 window around the beam. Three scintillation counters S_1, S_2, S_3 (in coincidence) and $\hat{C}, \bar{A}_1$ (in anticoincidence) were used for generating a *Start* signal of a fast programmable trigger unit.

Two scintillation counters S_1 and S_3, at a distance of 5.95 m, with double

side readout were used for time-of-flight measurements. The time-of-flight information and the amplitude of the second TOF counter (S_3) signal were used in a fast selection of a beam particle. The use of an anticoincidence counter around the beam behind the prototype and amplitude information from the second TOF counter permit suppressing multiparticle events resulting from beam particle interaction.

The *Start* signal synchronized by the mean-timed signal of the first TOF counter, and the mean-timed signal from the second TOF counter were sent to the first channel of a Memory Look Up (MLU) unit [5] for fast TOF measurement. The second channel of the MLU was used as a fast QDC of a linear sum of signals from both photomultipliers (EMI 9954-KB-03) of the second TOF counter.

The MLU is a programmable CAMAC module for fast two-dimensional (32×32) analysis. It has two fast 5-bit QDC and the RAM scheme. The memory contents can be controlled via a CAMAC bus. The address of the memory cell during the data taking is determined by the codes at the output of both QDC. The MLU generates a signal whenever the input TOF signals and the pulse height of the analog sum signal from the second TOF counter correspond to the requested particle (pion or proton in our case). This scheme provides a fast (100 ns) trigger and permits selection of particle species by changing "time" position of a mask. For rejection of multiparticle events inside the "window" of the anticoincidence counter the MLU unit was programmed to suppress events with a large amplitude of a signal in the S_3 counter.

Four output signals after the TOF constant fraction discriminators were sent to a TDC (Le-Croy 2228A) for off-line analysis.

The gas Cherenkov counter available on the T11 beam was used to veto positrons whose contents in the beam rapidly increases with decreasing momentum of the pion beam. Its efficiency is not known exactly, but taking into account the spectrum of the signals and the threshold of the discriminator we conclude that it should be higher than 90%. Besides that, positrons were additionally suppressed by more than 5 radiation lengths of material with the anticoincidence counter A_1 and the second TOF counter amplitude rejection. Residual positrons could be separated in part by TOF off-line analysis because at 0.7 GeV/c the pion beam has a delay about 0.4 ns (in our setup geometry) in comparison to relativistic positron. The measured time resolution of our TOF system was 0.23 ns for the pion beam.

2.1 LKr detector

The LKr detector consisting of a set of 8×12 cm^2 ionization chambers with a 2 cm gap was inserted into a cryostat of two coaxial stainless steel (316L) vessels. The inner one had a geometrical volume of 6.7 l. The chambers were

placed orthogonal to the beam axis. The chamber electrodes were made of FR4 (0.5 mm thick), covered on both sides with 18 μm copper layers. In total there were 9 electrodes alternatively connected to ground (5) and to high voltage (4). The first and the last signal electrodes with respect to the beam had pads of 8×8 cm^2, while the other three signal electrodes were divided into 10 mm wide strips in the x and y directions. One strip plane had double-side orthogonal strips. A delrin plastic support was used for the electrodes inside the cryostat. Before liquefaction of Kr the chamber was baked out for 2 days at about 60^{0}C.

We used no purification system for gaseous krypton since the industrial gas at our dispósal was already pure enough (electronegative impurities were expected to be below 1 ppm). Gaseous krypton flowed into the detector through a high purity stainless steel line at a pressure about 1.6 bar and was then liquefied by means of liquid nitrogen in a heat-exchange tube. To check the level of LKr during the liquefaction, the effect of increase in interelectrode capacitance due to dielectric constant of LKr was used. Voltage pulses were fed to the anodes and associated preamplifier signals were monitored while filling the prototype.

The temperature of liquid krypton was kept during the test at (-147±1.5)^{0}C and continuously monitored by 3 platinum resistor thermometers placed on the electrodes' support at different heights.

The five central strips in each plane and pads were connected to individual integrating preamplifiers; their output signals were sent to shaper-amplifiers with semi-gaussian shaping (τ_{sh}=500ns). The signals were digitized by a peak sensitive ADC (SILENA Mod. 4418/V) and then sent to a dedicated personal computer. The other parts of the signal electrodes were grounded. The shielded preamplifier box was mounted on the top flange of the cryostat. The preamplifiers were dc coupled to electrodes, each having a nominal feedback capacitance of 1 pF. For charge calibration, a voltage pulse from a precision pulse generator was injected into the preamplifiers through known test capacitors after each beam spill during the run.

Only the last 2 cm ionization chamber pad signal was used for this shape analysis. A signal from the preamplifier, based on FET SNJ-903L, of this pad channel was also sent after a wide band amplifier to a waveform digitizer (LeCroy Mod. 2262) with 40 MHz sampling frequency. This recorder has a 316 sample record length and a 10 bit resolution [6]. So we recorded the shape of the pad signal during a 7.9 μs time interval.

To reduce high frequency ripple in the high voltage a pair of passive low-pass filters were used.

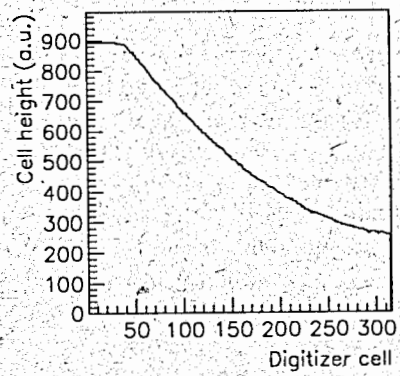

Figure 2: A typical digitized signal out of the preamplifier from the selected events

3 Data collection and selection

Data were taken for pions at momenta 580, 680 and 780 MeV/c and for protons at 1100, 1270 and 1440 MeV/c. Taking into account the energy loss of the particles, the beam momenta were set so as to have the data on ionization loss of the pions and the "kaons" at the entrance of the last gap at 500, 600 and 700 MeV/c. Total statistics of 15000 events was collected for these momenta, except for the calibration events. Data were also taken for different high voltages between the electrodes (0.5, 1.0, 2.5, 3.5 and 4.0 kV).

Unfortunately, we did not succeed in completely suppressing the external pickup noise, mainly caused by the power net. So some events were affected in this way, but part of these events had a distinguishable external influence, because of pulse nature of external pickup noise.

The events used in the analysis were selected according to the following OFF-LINE criteria:

1. a cut based on the TOF analysis (mean±0.4 ns);
2. a cut based on the second TOF counter signal amplitude analysis;
3. cuts on the pulse height of the total strip plane charge, and on (x, y) coordinates of the particle in the strip planes to reject multiparticle events, and to exclude current edge effect [2] (rejecting ≈58%);
4. cuts on the parameters of linear fit at the plateau before the signal, which is seen in Fig. 2 (rejecting ≈12%);
5. a cut based on the shape analysis of the signal itself in order to reject signals with distinguishable external noise influence (rejecting ≈13%).

About 13% of the events survived the cuts and were used for further analysis. Here we should give some comments on the last two cuts. The cuts in item 4 require a flat plateau before the signal, with a small slope and low value of χ^2 for linear fit. This permits one to reject events which are obviously affected by external pickup noise, or contain the tail of the previous signal. To make the cut on the basis of the shape analysis of the preamplifier output signal (item 5), the values of χ_i^2 for parabola fit for six overlapped parts of a signal were used. No cuts on the other parameters of the fit were imposed. Because such a cut is delicate and can affect the spectrum overlapping studied in our test, few threshold values of the χ_i^2 cutting were checked. The cut value which did not cause measurable change in the overlapping of ADC spectra of the shaped signals for two kinds of the particles was used for event rejection.

4 Data analysis

All data for shape analysis were taken at high voltage 3.5 kV. Fig. 3 shows the electric field dependence of the pulse height, taken in special samples, fitted by the formula [7]:

$$PH = \frac{C_q}{1 + E_0/E},$$

where C_q is the scale factor and E_0 is the recombination constant. The value obtained for the fitted parameter E_0 is (0.28±0.08) kV/cm. But here one should remember about the "ballistic" effect, because the decrease in the field strength causes the increase in the drift time. So at 0.5 kV/cm the fitted value is $T_{dr} \approx 10.7$ μs and the shaper ($2RC$-CR τ_{sh}=0.5 μs) signal amplitude is 10% smaller than that at 1.75 kV/cm with $T_{dr} \approx 7.2$ μs (see below).

The digitizer information of the selected "kaon" events at 0.5 GeV/c was analyzed to obtain the values of drift time (T_{dr}) and free electron lifetime (τ_e). This sample of events was chosen for analysis because of the smallest influence of energetic δ-electrons on the signal shape. Fig. 4 shows the spectra of these parameters fitted by the formula:

$$Q(t) = (-I_0 \cdot \tau_e + \frac{I_0}{T_{dr}} \cdot \tau_e \cdot t + \frac{I_0}{T_{dr}} \cdot \tau_e^2) \cdot exp(-\frac{t}{\tau_e}) + I_0 \cdot \tau_e - \frac{I_0}{T_{dr}} \cdot \tau_e^2 + C_0,$$

which is derived by integration of the expression $I(t) = I_0 \cdot (1 - t/T_{dr}) \cdot exp(-t/\tau_e)$ for $0 \le t \le T_{dr}$. The value of the drift time obtained from the fitting parameter histogram is T_{dr}=(7.2±0.04) μs (the error shown is statistical one). The systematic shift of this value estimated from comparison with Monte Carlo result (about −0.1 μs) is taken into account. As regards the meaning of τ_e its determination is more complicated because of the wide distribution of this parameter. This can be expected because the formula used for fitting does not take into

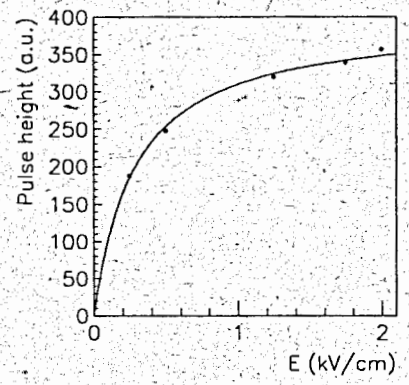

Figure 3: Field dependence of the pulse height. The curve is a fit to the data as described in the text

account non-uniform ionization distribution in a gap. To estimate the experimental value of τ_e, a decrease of the mean values of $dE/dx(i)_{mes}$ in different quasi-gaps was used (see below).

4.1 Shape analysis

The signal shape analysis of selected events was done in the following way. The set of samples during the drift time (starting at channel N∘. 45 in Fig. 2) was divided into few groups ($N_{gr} = 5 \div 8$), and the sum in each group was used for consecutive analysis. As a result of the first subtraction of one group contents from the contents of the next group, a set of $(N_{gr} - 1)$ values of the "current" was available. The second subtraction gave $(N_{gr} - 2)$ values of $dE/dx(i)_{mes}$ corresponding to the efficient number of quasi-gaps $N_{qg} = (N_{gr} - 2)$.

It is essential that the spectrum of $dE/dx(i)_{mes}$ for any i (the distribution of ionization in the quasi-gap with smaller thickness) differs from the ADC pulse height spectrum because of extension of the characteristic tail of the Landau distribution, though the electronic noise influence also increases. No measurable difference in the tail's characteristic for these spectra was found.

Because of limited value of τ_e the mean values of $dE/dx(i)_{mes}$ spectra for sequence of quasi-gaps decrease at some rate. This feature was used to estimate free electron lifetime.

For N_{qg}=4 the ratios of $dE/dx(n)_{mes}/dE/dx(4)_{mes}$ for $n = 2, 3, 4$ were used both for experimental data and for Monte Carlo events with the same values of T_{dr} and time duration of a group. The first spectrum of $dE/dx(1)_{mes}$ was not used because of systematic errors which can affect this mean value. This influence can be caused by the preamplifier or by some uncertainty in the start of the first group. Fig. 5 shows the experimental and simulated results. From this

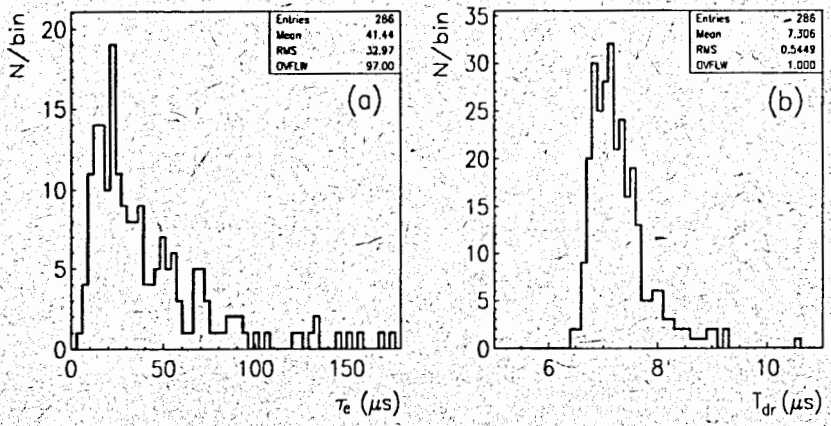

Figure 4: *a*) The parameters τ_e as the results of fitting of the experimental data; *b*) the histogram of the experimental data fitting parameter T_{dr}. Fitting was done for "kaon" events at 0.5 GeV/c

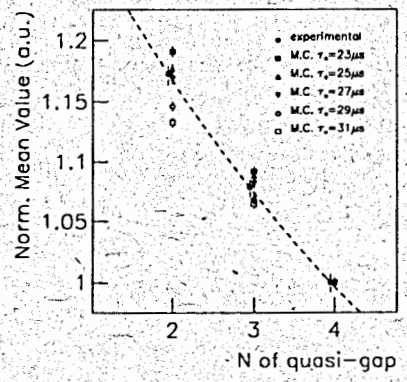

Figure 5: The normalized mean values of dE/dx in the sequence of the quasi-gaps for experimental data and for Monte Carlo simulated events (see the text)

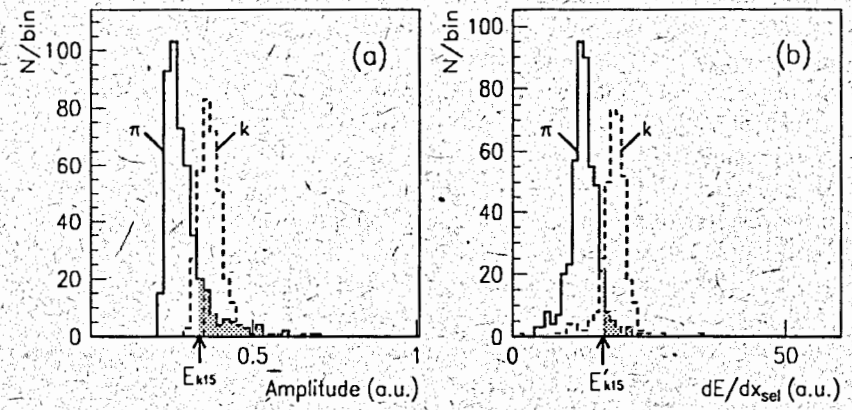

Figure 6: *a*) Height pulse spectra from ADC for the pion and "kaon" beams at 0.6 GeV/c (the digitizer signal specta are similar); *b*) dE/dx_{sel} after the selection described in the text. E_{k15} (E'_{k15})– threshold at which the left tail of "kaon" spectrum contains 15.83% of these particle events

analysis we concluded that the measured free electron lifetime is about 27 μs.

Taking into account the calibration data, we found that the measured charge from the 2 cm LKr chamber was about 2.84 times smaller than expected from calculation using W=20.5 eV/pair [1] and the free electron lifetime τ_e=27 μs. We concluded that this is caused by the recombination process. A similar result for non-purified krypton was mentioned in [8]. Although the "research grade" krypton with 0.1 ppm of O_2 was used, the charge response measured with the combined ^{207}Bi and ^{210}Po source in parallel plate chamber was less than 50% of the charge collected in the krypton after further purification. It is difficult to explain this result by short lifetime alone, because in this case it should be less than 3 μs, which contradicts our result and estimates in [9] for higher level of electronegative impurities in the gas.

As a measure of particle separation, the percentage of pions overlapped ($POO\%$) is used hereafter. It is equal to the ratio of the number of the particles in the left (pion) spectrum with deposited energy larger than E_{k15} (Fig. 6) to the total number of events in this spectrum. The meaning of E_{k15} is equal to the threshold value at which the left tail of the "kaon" energy spectrum contains 15.83% of the total number of "kaons", and it was determined for each particular case. This value is used because it is equal to half of the confidence level associated with 1σ deviation for the normal distribution. This measure of

separation permits analysis of spectra with the non-Gaussian shape.

At comparatively small free electron lifetime (Fig. 5) one should normalize different $dE/dx(i)_{mes}$ in each event to correct the systematic decrease of the "second derivative". The response of all quasi-gaps inside a gap should be identical in principle. Such normalization involving the cumulative distribution functions for particular spectra $dE/dx(i)_{mes}$ obtained for all data samples in our momentum range (0.5÷0.7 GeV/c) showed suitable result. But application of such normalization to the data at a particular momentum meaning permits one to improve results, although insignificantly. These values of $dE/dx(i)_{mes}$ for all events (at a certain momentum in the following analysis) were entered in the corresponding histograms (Fig. 7a, b), then cumulative distribution function for each quasi-gap was calculated (Fig. 7c, d). Fig. 7 depicts such normalization to the first quasi-gap spectrum for the fourth quasi-gap. In this case any systematic influence on the beginning of the signal shape is not so dangerous.

These values of $dE/dx(i)^n_{mes}$ for any event are different for a number of reasons: accidental appearance of δ-electrons along the track, the preamplifier electronic noise disturbance, and residual influence of the external pickup noise. A few ways [2] of exclusion of the quasi-gaps with large $dE/dx(i)^n_{mes}$ were tested in order to obtain the best separation of two spectra.

The resolution of the energy loss measurement, and therefore the separation of particles, using the method of the truncated mean [10] depend on the number of samples used. This dependence was studied by analyzing the mean values of 2 and 3 lowest quantities of $dE/dx(i)^n_{mes}$. Fig. 8(a, b) depicts the dependence of separation ($POO\%$) on the momentum of particles for few numbers of quasi-gaps (N_{qg}); then fixed numbers (2 and 3) of lowest $dE/dx(i)^n_{mes}$ were used for analysis. For comparison the $POO\%$ for amplitude spectra from ADC are also plotted; the curves are simple exponent fit lines.

Another method [2] of flexible rejection was studied by the experimental data analysis. It uses different numbers of selected values of $dE/dx(i)^n_{mes}$ in calculation of the mean value for each event. The following formula describes the number N_{mn} of the lowest values of $dE/dx(i)^n_{mes}$ used in calculation of dE/dx_{sel}:

$$N_{mn} = N_{qg} - IFIX\{k_s \cdot (N_{qg} - 1) \cdot (dE/dx_{max} - dE/dx_{min})/dE/dx_{min}\},$$

where dE/dx_{max} and dE/dx_{min} are maximal and minimal values of $dE/dx(i)^n_{mes}$. The minimal number of quasi-gaps taken into account was limited to $N_{mn} \geq 1$.

A few values of k_s, as is described in [2], were used for each value of the particle momentum. Then the optimal meaning of k_s was determined by analyzing the results at all 3 momentum values. The obtained values of k_s for different numbers of quasi-gaps happened to be in good agreement with the same parameters in Monte Carlo calculation.

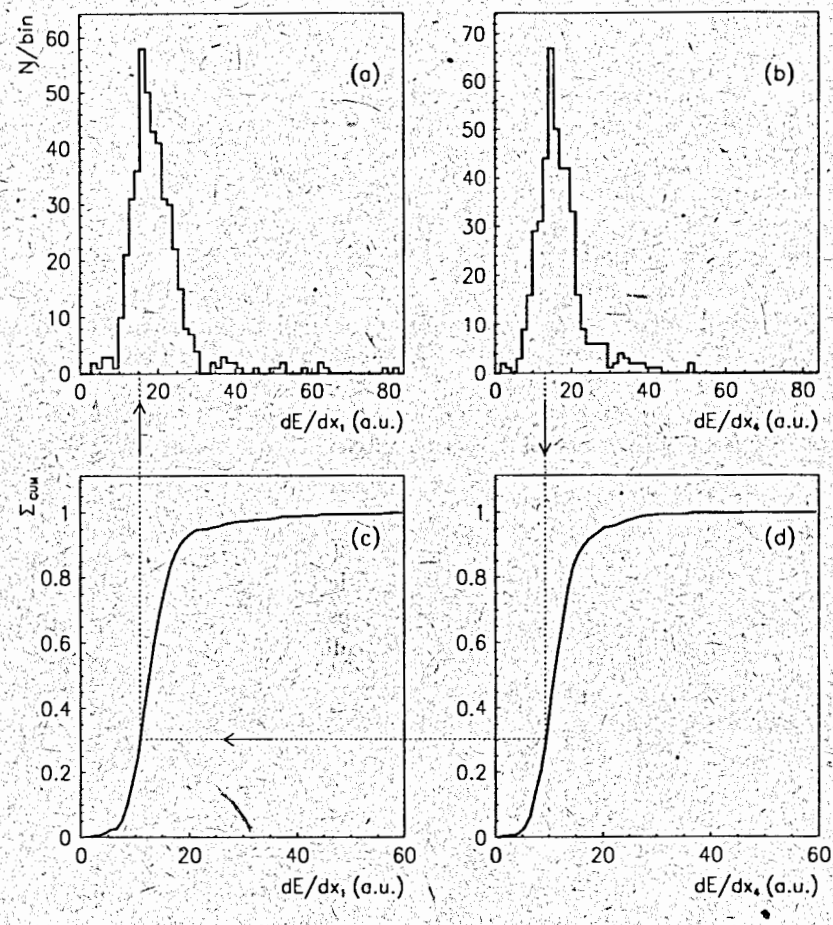

Figure 7: Normalization using cumulative distribution function for the "kaon" at 0.6 GeV/c. $dE/dx(1)_{mes}$ (a) and $dE/dx(4)_{mes}$ (b) spectra for selected events; cumulative distribution functions for the first (c) and fourth (d) quasi-gaps. The arrows show the sequence of using histograms in this algorithm

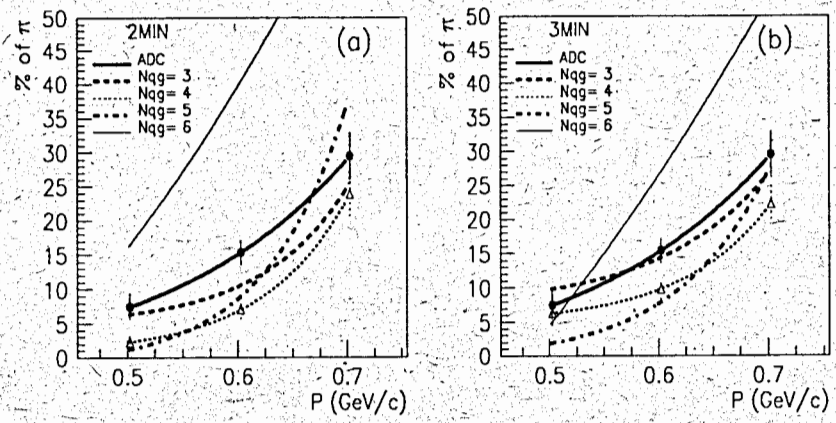

Figure 8: *a*) (π-k) particle separation (POO%) using 2 (*a*) or 3 (*b*) lowest $dE/dx(i)^n_{mes}$ in calculation of the mean values of the energy loss for different numbers of quasi-gaps

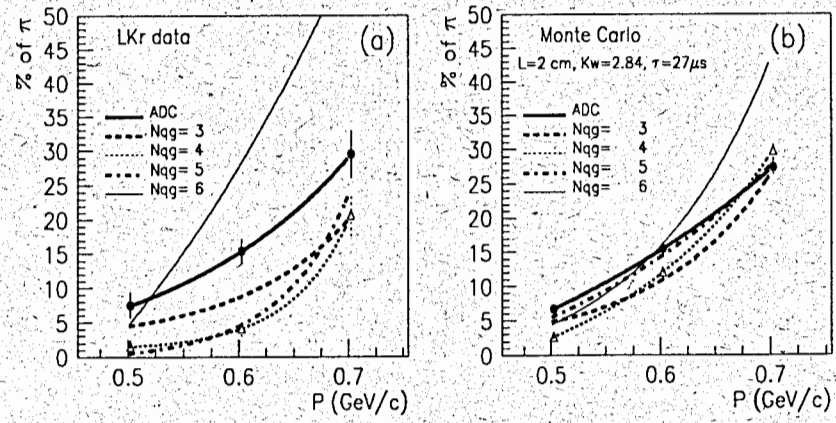

Figure 9: *a*) Experimental (π-k) particle separation (POO%) using the method of flexible rejection; *b)* Monte Carlo calculated particle (π-k) separation for similar parameters. Different curves correspond to different numbers of quasi-gaps. The errors are shown for ADC and N_{qg}=4 separation curves, for other cases the errors are roughly equal to corresponding values in the case of N_{qg}=4

Whith the method of flexible rejection (with varied number of N_{mn}),the particle separation for the same condition becomes better (Fig. 9*a*). For comparison Fig. 9*b* depicts the separation ability predicted from Monte Carlo calculation [2] for a 2 cm LKr chamber. The parameters of the charge loss, drift time and free electron lifetime were taken from our data analysis; the noise "amplitude" used in this calculation was 1 arbitrary unit (a.u.). It is obvious that the Monte Carlo predicted separation is worse than the experimental one. It became better if a lower noise level was used. The software noise generator used in [2] was designed by comparing the simulated result to a preamplifier noise characteristic when additional capacitance (C_{in}=82 pF) was attached to the input of the preamplifier. In our chamber test this capacitance was less than 30 pF. Besides that in the pad channel we used the selected preamplifier with the lowest value of the equivalent noise charge (ENC). The ENC measured in this test was about 595 electrons with shaper time constant τ_{sh}=0.5 μs. The expected increase in ENC due to additional capacitance C_{in}=50 pF seen by the preamplifier is about 150 electrons [11]. So this discrepancy in the separation capability can be explained by lower noise of the preamplifier used in this test.

5 Conclusion

The possibility of improving separation of π- and k-mesons in one gap of a liquid krypton uniform ionization chamber using the new method [2] is shown in experimental study. This method permits one to increase the boundary momentum of 2σ separation from 0.6 GeV/c up to 0.68 GeV/c. However, in our LKr chamber test the real signal was 2.84 times less than the predicted one. This resulted in degradation of the experimental separation capability compared to the calculated result. We concluded it is because of using non-purified krypton, as was mentioned in [8] (the twofold increase of signal was found after further purification of "research grade" Kr).

The comparison with the Monte Carlo result shows that software noise appears to be higher than the experimental noise of the preamplifier on the basis of the FET SNJ-903L transistor used in the study. This was due to lower value of detector capacitance than it was expected. Besides, the use of a preamplifier with lower noise would be desirable,too (the preamplifier used in this test was designed for high capacitance detector [11]). So one can hope to obtain the separation of π- and k-mesons at the level of 2σ in a 4 cm gap of purified LKr ionization chamber, as was predicted in [2].

The described new method of the signal shape analysis for rejection of energetic δ-electrons permits particle identification at fairly low momentum (see Fig.2 in [2]) depending on the property of the chamber. This method can be used in nuclear physics, where the signal-to-noise ratio would be higher for

particle with $Z > 1$. For particle separation by this method it is better to use a single-gap chamber (the first or the last gaps in a multiplane chamber), because for a double-gap chamber (as for internal gap in multiplane calorimeter) the separation capability becomes worse [2].

This method could be used if small thickness of detector is required, or if the time characteristics of a liquid medium chamber are studied.

From the analysis of two data samples taken at the beginning and at the end of the run we observed no measurable difference in the results. No degradation of krypton has been seen during the 7 days' run due to the materials (FR4, delrin, teflon cables, stainless steel 316L, soldering tin) used in the LKr detector construction.

References

[1] V.M. Aulchenko et al., Nucl. Instr. and Meth. A 316 (1992) 8.

[2] P.A. Kulinich, JINR Prep. E13-94-97, Dubna, 1994 (submitted to NIM).

[3] P. Cantoni et al., Nucl. Instr. and Meth. A 344 (1994) 156.

[4] U. Fano, Ann. Rev. Nucl. Sci. 13, 1 (1963).

[5] P.A. Kulinich, R. Toledo, JINR Prep. P10-87-112, Dubna, 1987.

[6] LeCroy Research Instrumentation Catalog, 1992.

[7] G. Jaffe, Ann. Phys., 42 (1913) 303.

[8] E. Aprile et al., Nucl. Instr. and Meth. A 327 (1993) 25.

[9] P.K. Lebedev, V.I. Pryanichnikov, Nucl. Instr. and Meth. A 327 (1993) 222.

[10] D. Jeanne et al., Nucl. Instr. and Meth. A 111 (1973) 287.

[11] V.M. Aulchenko et al., Nucl. Instr. and Meth. A 289 (1990) 468.

Received by Publishing Department
on June 3, 1994.